Supplementary Materials

Tuning hydride stability in TiVZrNb high-entropy hydrogen storage alloys via alloy-hydrogen electronegativity difference

Liangliang Zha[1,2], Liyuan Liu[3], Yihang Wang[1,2,3], Hongmei Cai[1,2], Yakun Zhang[1,2], Huijie Du[1,2,3], Bang Dou[2], Lufeng Xue[2], Yumeng Zhao[2], Di Wan[2,3], Yunfei Xue[1,2]

[1]School of Materials Science and Engineering, Beijing Institute of Technology, Beijing 100081, China.
[2]Yangtze Delta Region Academy of Beijing Institute of Technology, Jiaxing 314019, Zhejiang, China.
[3]School of Interdisciplinary Sciences, Beijing Institute of Technology, Beijing 100081, China.

Correspondence to: Prof. Di Wan, School of Interdisciplinary Sciences, Beijing Institute of Technology, Beijing 100081, China; Yangtze Delta Region Academy of Beijing Institute of Technology, Jiaxing 314019, Zhejiang, China. E-mail: diwan@bit.edu.cn. Prof. Yunfei Xue, School of Materials Science and Engineering, Beijing Institute of Technology, Beijing 100081, China; Yangtze Delta Region Academy of Beijing Institute of Technology, Jiaxing 314019, Zhejiang, China. E-mail: xueyunfei@bit.edu.cn

Supplementary Figures

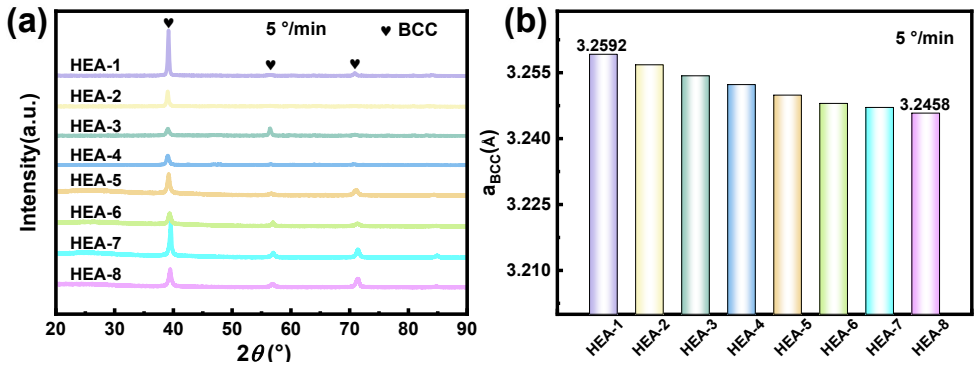

Supplementary Figure 1. (a) XRD patterns of HEA-1 to HEA-8 collected at a scan rate of 5°/min; (b) corresponding lattice parameters obtained by GSAS-II refinement.

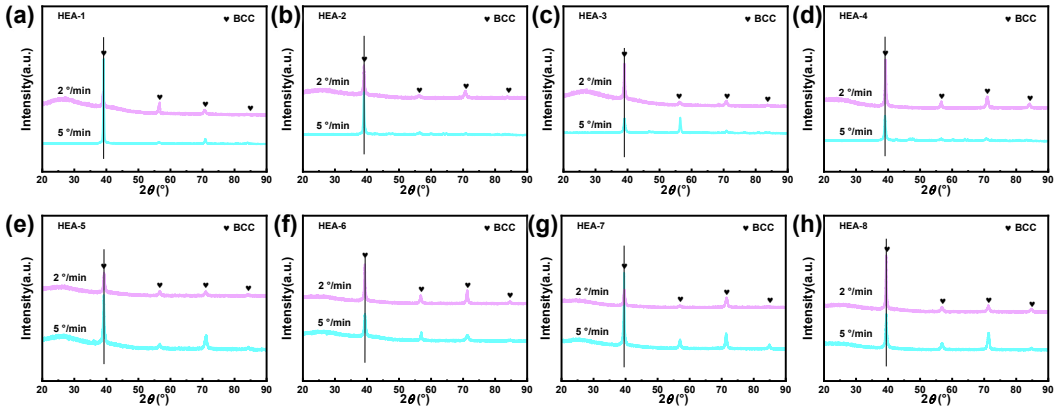

Supplementary Figure 2. Comparison of XRD patterns of HEA-1 to HEA-8 collected at scan rates of 5°/min and 2°/min: (a) HEA-1, (b) HEA-2, (c) HEA-3, (d) HEA-4, (e) HEA-5, (f) HEA-6, (g) HEA-7, and (h) HEA-8.

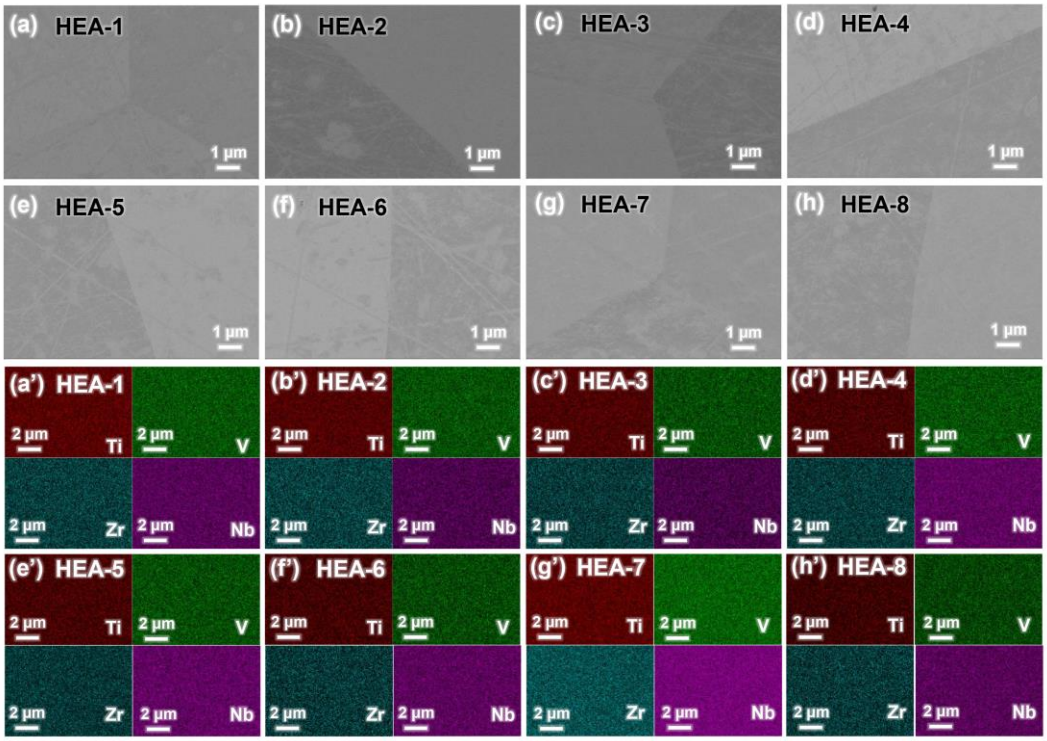

Supplementary Figure 3. The higher-magnification BSE images (a-h) and the corresponding EDS maps (a'-h') of HEA-1 to HEA-8 alloys.

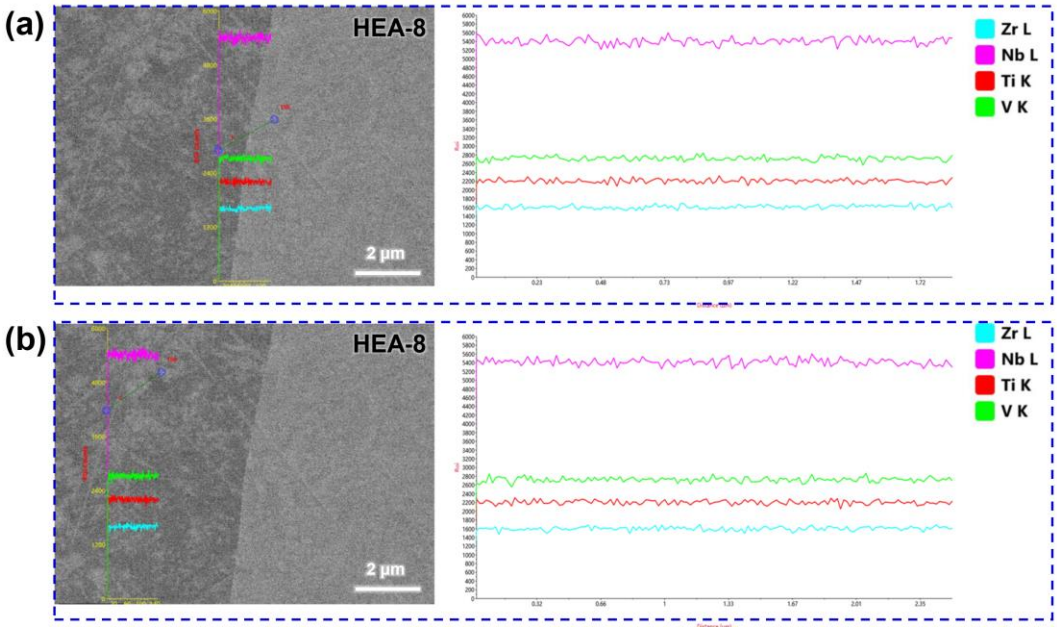

Supplementary Figure 4. EDS line-scan results of the HEA-8 alloy: (a) grain boundary region and (b) grain interior region.

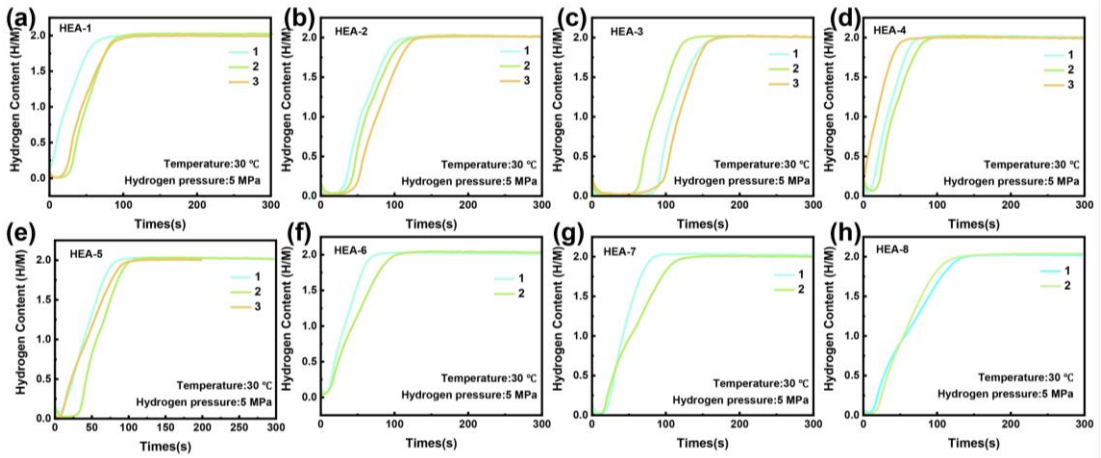

Supplementary Figure 5. Repeated initial hydrogen absorption kinetics curves of activated HEA-1 to HEA-8 measured at 303 K and 5 MPa hydrogen pressure: (a) HEA-1, (b) HEA-2, (c) HEA-3, (d) HEA-4, (e) HEA-5, (f) HEA-6, (g) HEA-7, and (h) HEA-8. These repeated measurements were used to calculate the standard deviations of the H/M values, which are shown as error bars in Figure 5b.

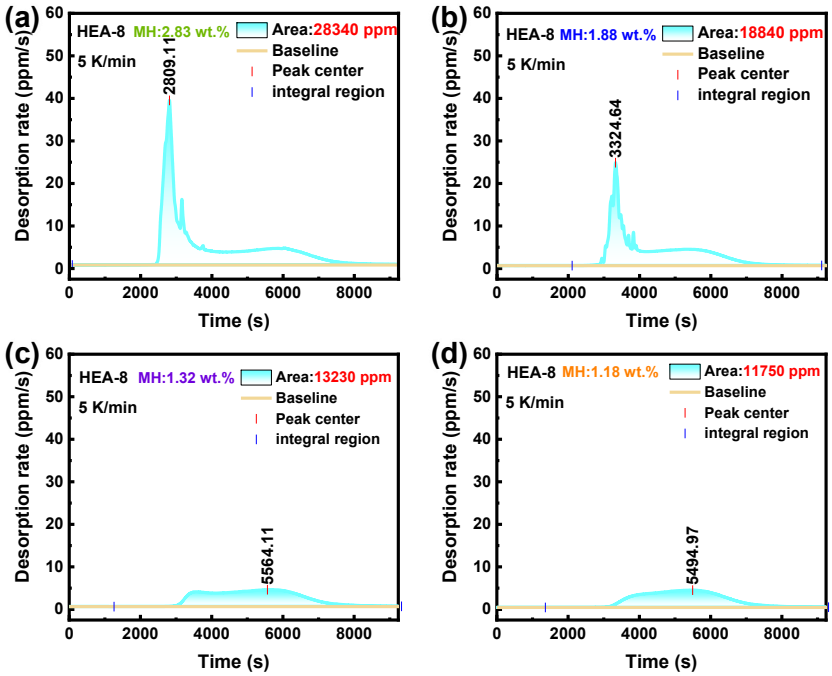

Supplementary Figure 6. TDS hydrogen desorption curves and corresponding integration results of the HEA-8 alloy with different hydrogen contents: (a) 2.83 wt.%, (b) 1.88 wt.%, (c) 1.32 wt.%, and (d) 1.18 wt.%.

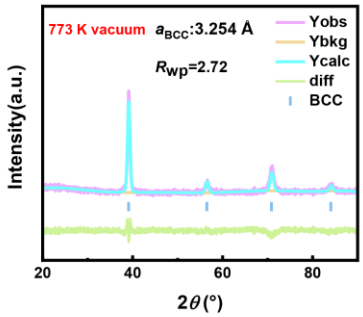

Supplementary Figure 7. XRD pattern of the HEA-8 alloy after dynamic vacuum dehydrogenation at 773 K for 1 h.

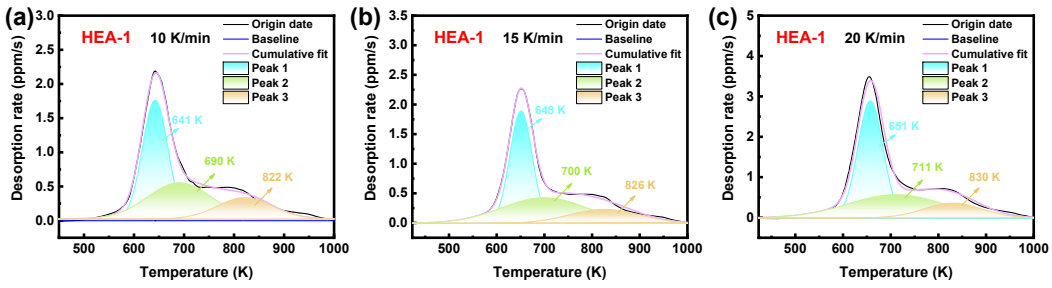

Supplementary Figure 8. TDS hydrogen desorption curves and corresponding

Gaussian peak deconvolution results of the HEA-1 alloy at different heating rates: (a) 10 K/min, (b) 15 K/min, and (c) 20 K/min.

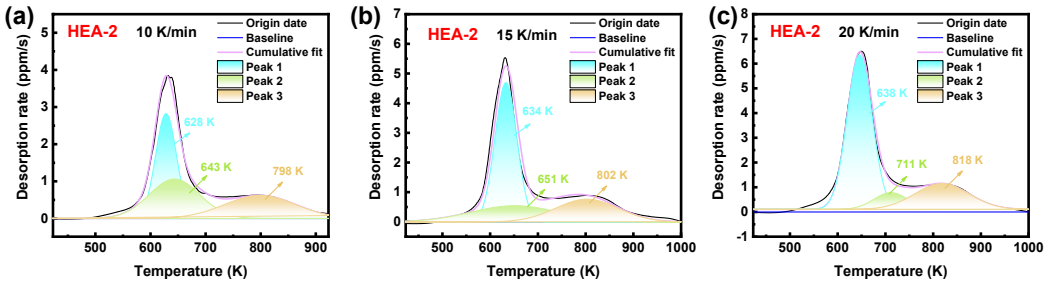

Supplementary Figure 9. TDS hydrogen desorption curves and corresponding Gaussian peak deconvolution results of the HEA-2 alloy at different heating rates: (a) 10 K/min, (b) 15 K/min, and (c) 20 K/min.

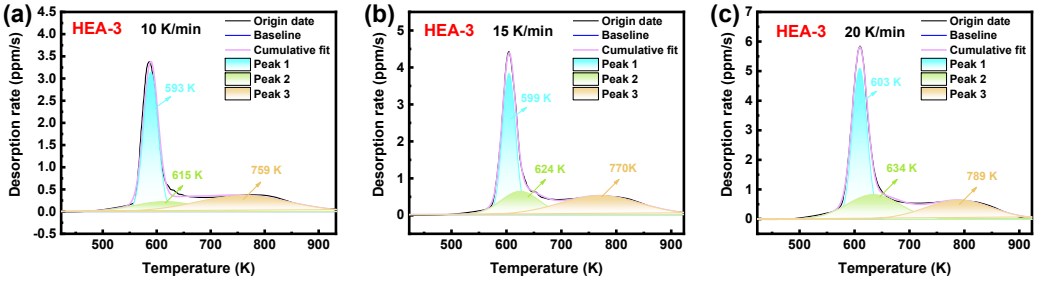

Supplementary Figure 10. TDS hydrogen desorption curves and corresponding Gaussian peak deconvolution results of the HEA-3 alloy at different heating rates: (a) 10 K/min, (b) 15 K/min, and (c) 20 K/min.

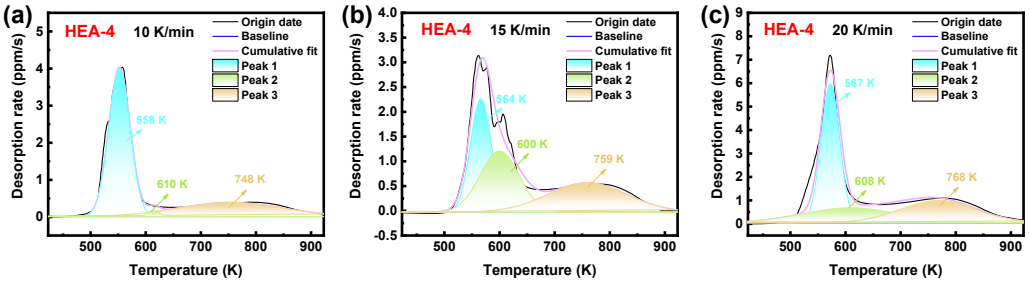

Supplementary Figure 11. TDS hydrogen desorption curves and corresponding Gaussian peak deconvolution results of the HEA-4 alloy at different heating rates: (a) 10 K/min, (b) 15 K/min, and (c) 20 K/min.

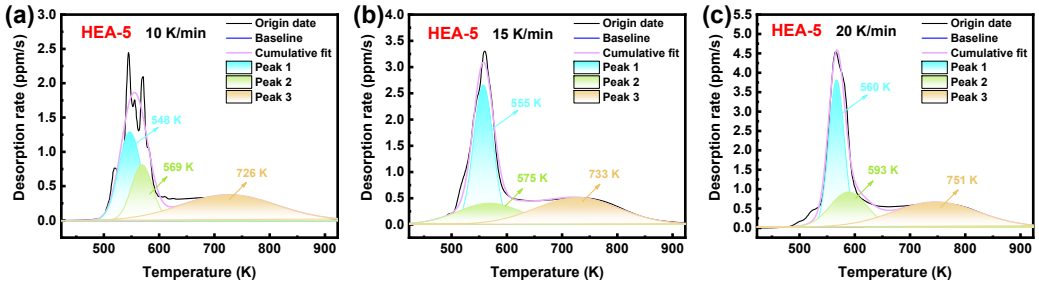

Supplementary Figure 12. TDS hydrogen desorption curves and corresponding Gaussian peak deconvolution results of the HEA-5 alloy at different heating rates: (a) 10 K/min, (b) 15 K/min, and (c) 20 K/min.

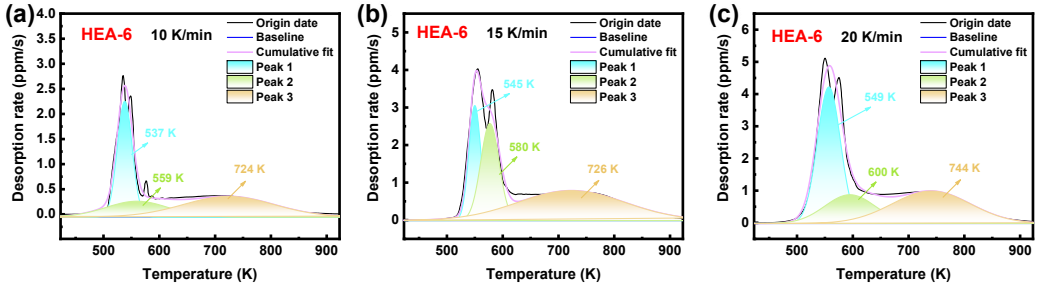

Supplementary Figure 13. TDS hydrogen desorption curves and corresponding Gaussian peak deconvolution results of the HEA-6 alloy at different heating rates: (a) 10 K/min, (b) 15 K/min, and (c) 20 K/min.

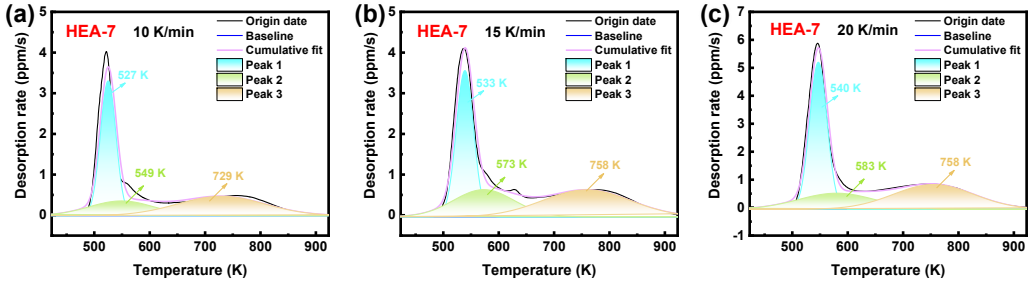

Supplementary Figure 14. TDS hydrogen desorption curves and corresponding Gaussian peak deconvolution results of the HEA-7 alloy at different heating rates: (a) 10 K/min, (b) 15 K/min, and (c) 20 K/min.

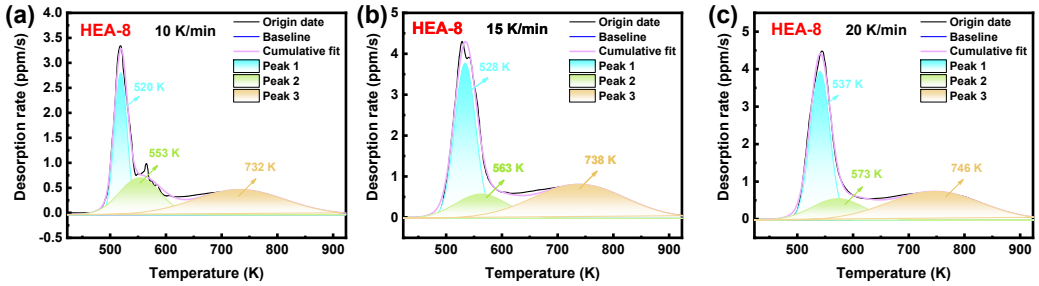

Supplementary Figure 15. TDS hydrogen desorption curves and corresponding Gaussian peak deconvolution results of the HEA-8 alloy at different heating rates: (a) 10 K/min, (b) 15 K/min, and (c) 20 K/min.

Supplementary Tables

Supplementary Table 1. The atomic radius (*r*), *VEC*, and Pauling electronegativity (χ^P) of the elements are involved

Element	*r* [Å]	VEC	χ^P
H	-	-	2.20
Ti	1.462	4	1.54
V	1.316	5	1.63
Zr	1.603	4	1.33
Nb	1.429	5	1.60
Mo	1.363	6	2.16
Cr	1.249	6	1.66
Fe	1.241	8	1.83
Mn	1.350	7	1.55

Supplementary Table 2. Atomic ratios and lattice constants for alloys HEA-1 to HEA-8

Alloy	Composition	*a* (Å)	
		5 °/min	2 °/min
HEA-1	$Ti_{40}V_{30}Zr_{10}Nb_{20}$	3.2592(5)	3.2594(5)
HEA-2	$Ti_{35}V_{30}Zr_{10}Nb_{25}$	3.2568(4)	3.2568(4)
HEA-3	$Ti_{30}V_{30}Zr_{10}Nb_{30}$	3.2543(4)	3.2543(4)
HEA-4	$Ti_{25}V_{30}Zr_{10}Nb_{35}$	3.2523(5)	3.2521(5)
HEA-5	$Ti_{27.5}V_{30}Zr_{7.5}Nb_{35}$	3.2499(4)	3.2499(4)

HEA-6	$Ti_{30}V_{30}Zr_5Nb_{35}$	3.2480(4)	3.2480(4)
HEA-7	$Ti_{27.5}V_{30}Zr_5Nb_{37.5}$	3.2471(4)	3.2470(4)
HEA-8	$Ti_{25}V_{30}Zr_5Nb_{40}$	3.2458(4)	3.2458(4)

Note: The values in parentheses represent the standard uncertainties in the last digit obtained from GSAS-II refinement.

Supplementary Table 3. Actual PCT test temperatures used for Van't Hoff analysis, hydrogen absorption/desorption plateau pressures, and enthalpy changes of HEA-1 to HEA-8 alloys

Sample	Temp.[K]	Pressure [MPa]		ΔH [kJ/mol H_2]		Van't Hoff fitting parameters-*p value*	
		Ab.	De.	Ab.	De.	Ab.	De.
HEA-1	496	0.184	0.017	-219.5±6.73	230.3±6.82	0.0020	0.0218
	506	0.527	0.053				
	512	0.966	0.095				
HEA-2	489	0.200	0.015	-208.7±7.89	222.0±3.24	0.0493	0.0333
	499	0.630	0.050				
	507	1.228	0.106				
HEA-3	486	0.384	0.026	-207.0±2.82	208.7±2.25	0.0597	0.0070
	498	1.539	0.088				
	506	2.845	0.200				
HEA-4	481	0.309	0.023	-193.7±6.65	177.1±3.74	0.0492	0.0136
	493	1.155	0.064				
	503	2.555	0.157				
HEA-5	467	0.155	0.012	-180.4±4.49	160.5±6.48	0.0394	0.0300
	475	0.307	0.022				
	485	0.862	0.053				
HEA-6	457	0.092	0.007	-162.1±8.06	141.3±4.99	0.0350	0.0025
	467	0.251	0.016				
	477	0.553	0.034				
HEA-7	449	0.256	0.012	-101.4±5.74	122.2±4.32	0.0364	0.0225
	457	0.433	0.02				

	466	0.690	0.039				
	421	0.063	0.004				
HEA-8	438	0.194	0.011	-93.9±5.15	97.3±1.99	0.0353	0.0130
	453	0.417	0.027				

Notes: The temperatures listed in this table are the actual PCT test temperatures used for the Van't Hoff fitting. The first extremely low-pressure plateau associated with the highly stable β-hydride phase was not included in the Van't Hoff fitting. The listed plateau pressures correspond to the main measurable absorption/desorption plateau related to the practical reversible hydrogen storage capacity. The plateau pressures were obtained from the middle region of the measurable main absorption/desorption plateau. The 303 K PCT curves shown in Figure 6 were used only to illustrate the initial hydrogen absorption behavior and capacity characteristics and were not included in the Van't Hoff analysis. The uncertainties of ΔH_{abs} and ΔH_{des} were calculated from the standard errors of the slopes in the Van't Hoff linear fittings performed using Origin.

Supplementary Table 4. Peak temperatures obtained from Gaussian deconvolution of TDS curves at different heating rates and apparent activation energies of Peak1 for HEA-1 to HEA-8 alloys

Sample	**Peak**	**Peak temperature (K)**				***E_a*** **(kJ/mol)**
		5 K/min	**10 K/min**	**15 K/min**	**20 K/min**	
	1	632	641	648	651	232.21±4.39
HEA-1	2	681	690	700	711	
	3	810	822	826	830	
	1	619	628	634	638	228.21±5.64
HEA-2	2	621	643	651	711	
	3	789	798	802	818	
	1	585	593	599	603	214.75±8.38
HEA-3	2	595	615	624	634	
	3	722	759	770	789	
HEA-4	1	549	558	564	567	186.4±8.97

	2	573	610	600	608	
	3	725	748	759	768	
	1	541	548	555	560	171.93±8.89
HEA-5	2	558	569	575	593	
	3	720	726	733	751	
	1	528	537	545	549	146.5±7.73
HEA-6	2	547	559	580	600	
	3	722	724	726	744	
	1	516	527	533	540	127.62±6.40
HEA-7	2	540	549	573	583	
	3	720	729	758	758	
	1	509	520	528	537	105.01±3.74
HEA-8	2	533	553	563	573	
	3	723	732	738	746	

Note: Only the deconvoluted Peak 1 temperatures were used for Kissinger fitting; therefore, E_a values are reported only for Peak 1. The fitting uncertainties of E_a were calculated from the standard errors of the slopes in the Kissinger linear fittings.